Variations in Finite Difference Potential Fields

Predictive Science Inc.

Ronald M. Caplan, Cooper Downs, and Jon A. Linker

Predictive Science Inc. 9990 Mesa Rim Rd San Diego, CA 92121 www.predsci.com

INTRODUCTION

The potential field (PF) solution of the solar corona is a vital modeling tool for a wide range of applications, including minimum energy estimates, coronal magnetic field modeling, and deriving empirical solar wind solutions. However, various methods for computing PFs can yield different solutions, hindering, at times, their proper application. Even for a given computational method, differences in the solution can occur depending on the boundary conditions, resolution, and model parameters. Here we study PF solutions centered on 2012-06-13:13:11:36 TAI using our finite difference code POT3D.

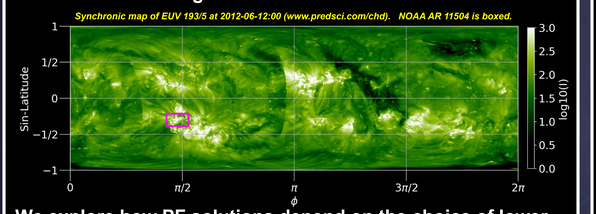

We explore how PF solutions depend on the choice of lower boundary conditions (the input magnetogram), upper boundary conditions (e.g. source-surface radius), and resolution of the calculation. The PF solutions are analyzed both globally and localized near NOAA AR 11504.

POT3D

$$\nabla^2\Phi = 0$$
$$\vec{B} = \nabla\Phi$$

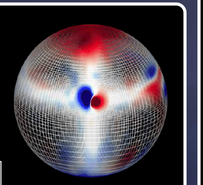

Finite-difference potential field solver on a non-uniform logically-rectangular three-dimensional spherical grid.

$$\nabla^2\Phi_{i,j,k} \approx \frac{1}{\Delta r_i}\left[\frac{\Phi_{i+1,j,k}-\Phi_{i,j,k}}{\Delta r_{i+\frac{1}{2}}} - \frac{\Phi_{i,j,k}-\Phi_{i-1,j,k}}{\Delta r_{i-\frac{1}{2}}}\right]$$
$$+\frac{1}{\sin\theta_j\,\Delta\theta_j}\left[\sin\theta_{i,j+\frac{1}{2}}\frac{\Phi_{i,j+1,k}-\Phi_{i,j,k}}{\Delta\theta_{j+\frac{1}{2}}} - \sin\theta_{i,j-\frac{1}{2}}\frac{\Phi_{i,j,k}-\Phi_{i,j-1,k}}{\Delta\theta_{j-\frac{1}{2}}}\right]$$
$$+\frac{1}{\sin^2\theta_j\,\Delta\phi_k}\left[\frac{\Phi_{i,j,k+1}-\Phi_{i,j,k}}{\Delta\phi_{k+\frac{1}{2}}} - \frac{\Phi_{i,j,k}-\Phi_{i,j,k-1}}{\Delta\phi_{k-\frac{1}{2}}}\right] = 0$$

Lower boundary condition set by photospheric magnetic field data: $\left.\frac{\partial\Phi}{\partial r}\right|_{R_\odot} = \left.B_r\right|_{R_\odot}$

Upper radial boundary condition options:

Closed-wall: $\left.\frac{\partial\Phi}{\partial r}\right|_{r_1} = 0$

Source-surface: $\left.\Phi\right|_{r_{ss}} = 0$

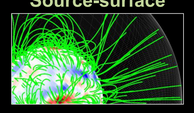

Polar boundary conditions set using average: $\left.\Phi\right|_{\theta_{0/\pi}} = \frac{1}{2\pi}\int_{\phi=0}^{\phi=2\pi}\left.\Phi\right|_{\theta_{0/\pi}\pm\epsilon}\,d\phi$

Solution computed with a sparse-matrix preconditioned conjugate gradient solver

Written in FORTRAN and parallelized for use with multiple CPUs and GPUs using MPI+OpenACC [arXiv:1709.01126]

FORTRAN MPI OpenACC

Available for use as part of the WSA model in the CORHEL suite at CCMC

Community Coordinated Modeling Center

MAP PREPARATION

(1) Combine HMI CR and SHARP data. **(2)** Add polar data of random localized parasitic polarities with total flux matching HMI-derived values

(3) Interpolate to desired resolution preserving flux and **(4)** flux-balance through selective multiplication

(5) Smooth map using spherical surface diffusion with a grid-based local viscosity

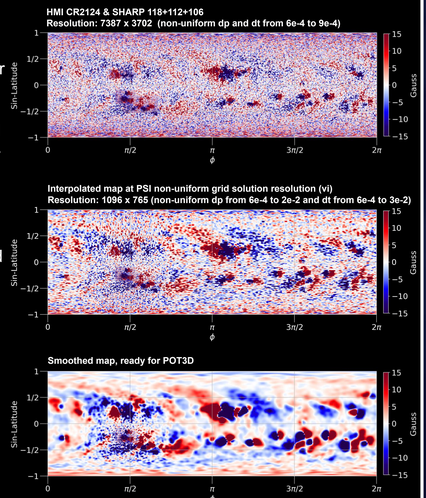

For ready-made pole-filled maps, only need steps **(3)** - **(5)**

DEFAULT RUN INFORMATION: All runs use a radial non-uniform grid that coarsens towards the outer boundary. Unless otherwise specified, all runs use a source-surface outer radial boundary condition at $r_{ss} = 2.5$ and the PSI input map (f) interpolated to a uniform 360x180 resolution (ii). The AR11504 post-analysis bounding box is defined by: $r \in [1.0, 1.2]$ $\theta \in [1.79, 1.93]$ $\phi \in [1.37, 1.65]$

VARIATIONS IN BOUNDARY CONDITIONS

(1) Closed-wall $r_1 = 2.5$
(2) Source-surface $r_{ss} = 1.5$
(3) Source-surface $r_{ss} = 2.0$
(4) Source-surface $r_{ss} = 2.5$

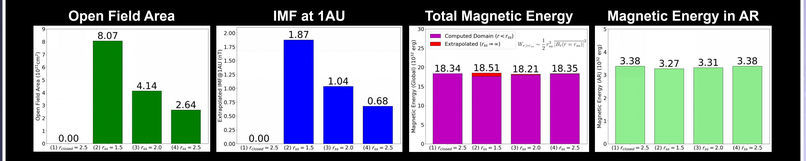

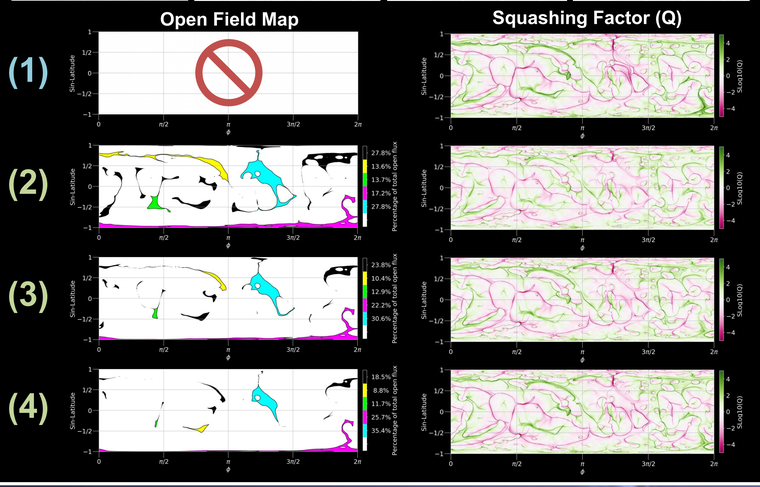

VARIATIONS IN RESOLUTION

```
(i)   Tiny:    (Uniform  90x 180)x(r: 27) [  0.4 million cells]
(ii)  Small:   (Uniform 180x 360)x(r: 54) [  3.5 million cells]
(iii) Medium:  (Uniform 450x 900)x(r:135) [ 54.7 million cells]
(iv)  Large:   (Uniform 900x1800)x(r:207) [335.3 million cells]
(v)   Native:  (Non-uniform Native SHARP to Native HMI 2012x3973)x(r:827)
               [  6.6 billion cells]
(vi)  PSI:     (Non-uniform Native SHARP to Small (ii)  742x1095)x(r:216)
               [175.5 million cells]
```

VARIATIONS IN INPUT DATA

(a) Synoptic CR
(b) Hourly 11:54
(c) Janis 11:54
(d) Synoptic CR
(e) Daily 12:00
(f) PSI [(d)+SHARP+Pole]

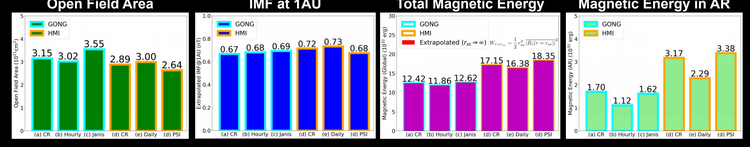

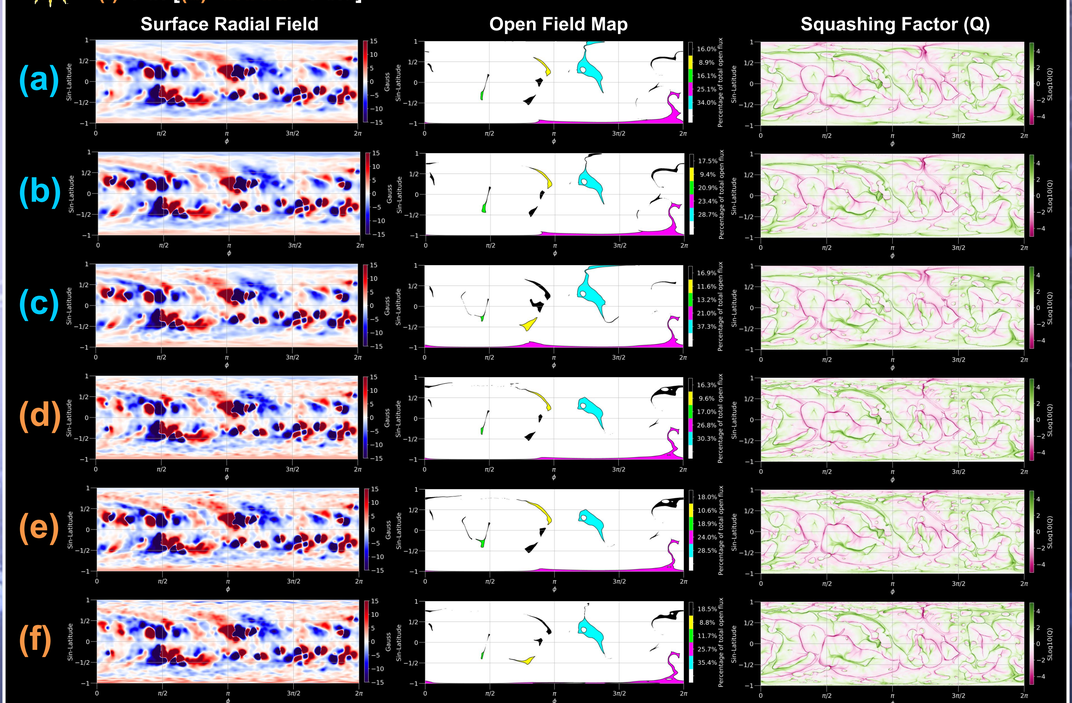

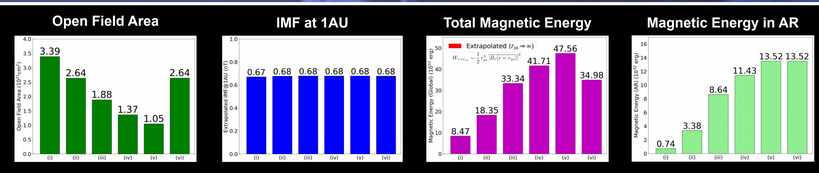

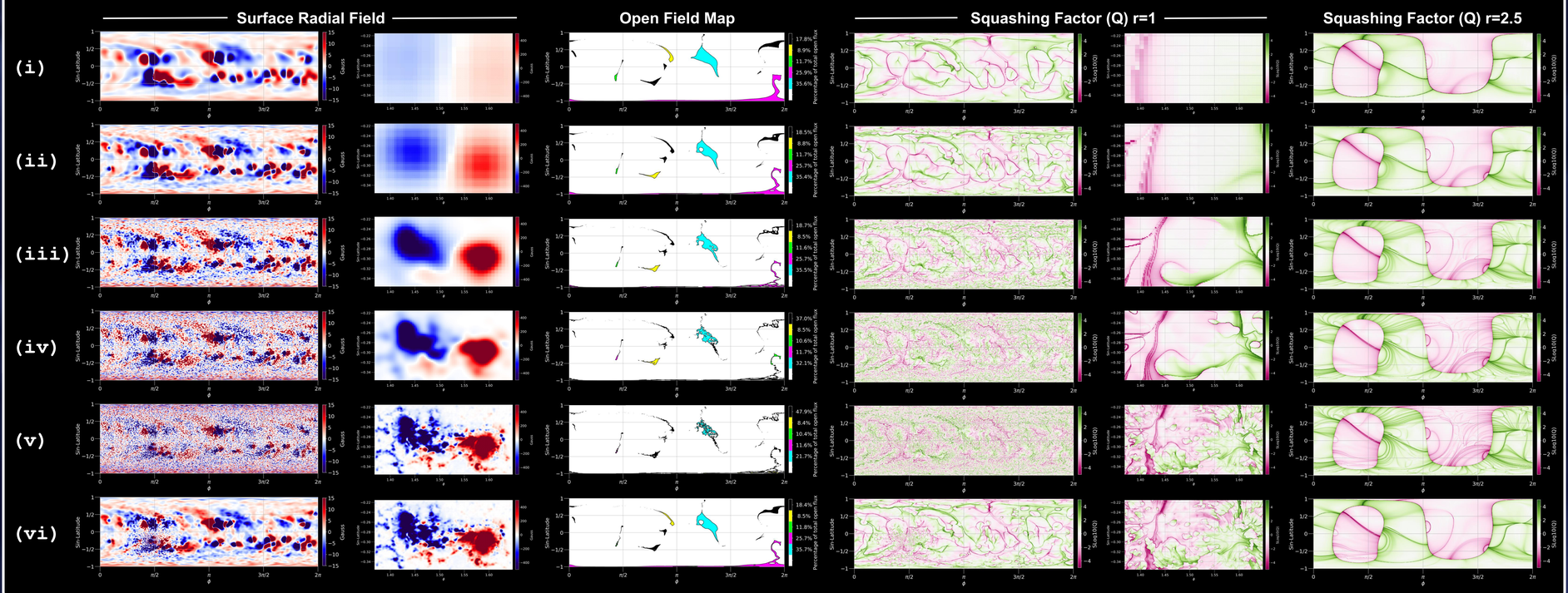

COMPUTATIONAL PREFORMANCE

Uniform vs. Non-uniform grid centered at active region:

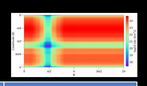

Resolution	Wall Clock Time
(v) Native (6.6 billion cells)	871 seconds
(vi) PSI (175 million cells)	18 seconds

Computational Environment:
XSEDE TACC Stampede 2
120 Dual-socket 24-core Intel Skylake Platinum 8160 Nodes (5760 total cores)

~50x Speedup!

Single-server CPU and GPU timing results:

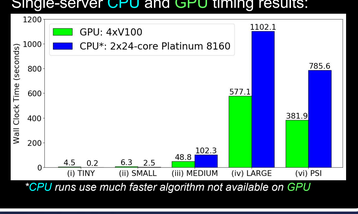

*CPU runs use much faster algorithm not available on GPU

DISCUSSION

- Changes between input data has only a small effect on the total open flux, but more of an effect on magnetic energy and topology, especially in the active region (AR).
- Outer boundary conditions have nearly no effect on magnetic energy, but a very large effect on the open flux and open field structure.
- Changes in resolution have nearly no effect on the open flux, but a large effect on magnetic energy and structure.
- Using a non-uniform grid to capture an AR at high resolution is much faster to compute than using an equivalent uniform grid, and does not alter the structure or derived quantities in the vicinity of the AR.

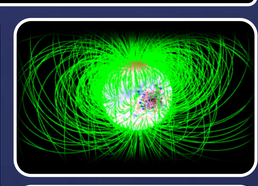

Funding provided by

NASA NSF